Published in final edited form as:
Biochemistry. 2011 March 29; 50(12): 1963–1965. doi:10.1021/bi2000824.

Residue-specific Fluorescent Probes of α-Synuclein: Detection of Early Events at the N- and C-termini during Fibril Assembly†

Thai Leong Yap, **Candace M. Pfefferkorn**, and **Jennifer C. Lee***
Laboratory of Molecular Biophysics, National Heart, Lung, and Blood Institute, National Institutes of Health, Bethesda, Maryland 20892

Abstract

In the Parkinson's disease-associated state, α-synuclein (α-syn) undergoes large conformational changes forming ordered, β-sheet containing fibrils. To unravel the role of specific residues during the fibril assembly process, we prepared single-Cys mutants in the disordered (G7C and Y136C) and proximal (V26C and L100C) fibril core sites and derivatized them with environment sensitive dansyl (Dns) fluorophores. Dns fluorescence exhibits residue-specificity in spectroscopic properties as well as kinetic behavior; early kinetic events were revealed by probes located at positions 7 and 136 compared to those positioned at 26 and 100.

α-Synuclein (α-syn) is a 140 residue, cytoplasmic and membrane-associated human protein that is highly expressed in presynaptic nerve terminals (1). Though it is linked to numerous physiological roles (2), α-syn is most well known for its connection to amyloid (fibril) formation (3) and its presence in Lewy bodies, the pathological hallmark of Parkinson's disease (1). This filamentous material contains ordered β-strands, aligned perpendicular to the fibril axis (4–7).

Established by various experimental approaches, the α-syn fibril core consists of residues 30 – 100 with disordered N- and C-terminal regions (Figure 1a) (8–11). While outside the amyloid core, in the soluble state, the N- and C-termini participate in intra- and inter-molecular interactions (12–14). Fluorescence spectroscopy has been effective for studying α-syn conformation (15–18) and aggregation (19–24); however, kinetic details at the residue level during amyloid formation remain limited. Towards this objective, we sought to define residue-specific behaviors of the N- *versus* C-terminus during protein aggregation by introducing environmentally-sensitive dansyl (Dns) (25) fluorescent probes at multiple sites (Figure 1b).

We prepared four single-Cys α-syn mutants in the disordered (G7C and Y136C) and proximal fibril core sites (V26C and L100C) at N- and C-terminal regions and derivatized them with the thiol-reactive Dns precursor, 5-((((2-iodoacetyl)amino)ethyl)amino)-naphthalene-1-sulfonic acid. Minimal Dns-protein (1.5%) was used to monitor wild-type (WT) protein aggregation (1.5 μM Dns-protein and 100 μM WT). Because α-syn fibril formation generally exhibits sigmoidal kinetics, we made frequent fluorescence and laser

†Supported by the Intramural Research Program at the National Heart, Lung, and Blood Institute, National Institutes of Health.

*To whom the correspondence should be addressed to. leej4@mail.nih.gov. Tel: 301-496-3741. Fax: 301-402-3404.

SUPPORTING INFORMATION AVAILBLE.

Supplementary figures, tables, and detailed experimental methods. This material is free of charge via the Internet at http://pubs.acs.org.

light scattering (LS) measurements during the lag, exponential growth, and mature phases (Figure 1c, d) (26–28).

Similar to the WT protein, we find that Dns-labeled proteins are predominantly disordered in solution, adopt helical structure in the presence of sodium dodecyl sulfate micelles (29), and form β-sheets upon aggregation (Figures S1,2) (30). Consistent with the circular dichroism data for the soluble protein, steady-state and excited-state fluorescence properties of the Dns probe were site independent, reflecting water-exposed fluorophores (mean wavelength, $\langle\lambda\rangle \sim 525 – 528$ nm, Table S1, average excited state lifetime, $\langle\tau\rangle \sim 10$ ns, data not shown). In addition, morphology of fibrils containing mixtures of WT and Dns-labeled proteins is indistinguishable from WT alone (Figure S3). Using N-acetylcysteine derivative of Dns, we ascertained that the fluorophore itself is not a fibril probe (Figure S4). These results show that the Dns-labeled proteins are not measurably different from the WT protein alone and can be used as reporters of α-syn amyloid formation.

Upon aggregation, Dns fluorescence exhibits dramatic spectroscopic and residue-specific sensitivity (Figures 1c, S5). We observe overall intensity increases (1.6 – 3 fold) and spectral blue shifts ($\Delta\langle\lambda\rangle = 16 – 42$ nm) indicating that all Dns sites are sequestered from an aqueous to a more hydrophobic local environment. Unexpectedly, Dns7 and Dns136 ($\Delta\langle\lambda\rangle = 42$ and 29 nm, respectively), residues outside the amyloid core were more responsive probes than that of residues proximal to the core, Dns26 and Dns100 ($\Delta\langle\lambda\rangle = 16$ and 20 nm, respectively); Dns7 is in the most hydrophobic surrounding whereas Dns26 and Dns100 appear to be markedly more polar. Anisotropy and fluorescence decay data also show increased immobilization (Table S1) and lifetimes ($\langle\tau\rangle \sim 12 – 16$ ns, data not shown).

To assess whether Dns probes are sensitive to early aggregation events (23,24), kinetics derived from $\langle\lambda\rangle$ were compared to LS measurements which report on macroscopic aggregates (size detection limit ≥ 100 nm). From independent experiments, we confirmed that similar midpoint transitions were obtained for LS and the standard thioflavin T (ThT) assay in detecting fibril formation (Figure S6). Because of inherent sample-to-sample variations in the lag phase (31), during which time little changes in fibril concentration can be detected, we elected to present a full representative data set for the mixture of WT and Dns136 (Figure 1d) to exemplify that despite the uncertainties in the lag times (20 – 30 h), spectroscopic data ($\langle\lambda\rangle$) and respective trend [$t_{50}(\Delta\langle\lambda\rangle)$ *vs.* t_{50}(LS), the midpoint transition times] are consistent and reproducible (see Figure S7 for other sites). To ascertain that the Dns probe has little effect on WT aggregation kinetics, we performed concentration dependence studies (1.5 – 9 μM Dns136) and found no apparent differences (Figure S8). We note that while a variety of fluorophores can be chosen for and used to probe α-syn aggregation, larger, more hydrophobic molecules can perturb the kinetics (21,23,24).

When monitored by Dns fluorescence, both Dns7 and Dns136 exhibit earlier aggregation kinetics compared to Dns26 and Dns100 (Figure S7). Additionally, Dns7- and Dns136-monitored kinetics preceded the LS curves whereas in contrast, nearly identical behaviors were found for Dns26 and Dns100 compared to that of LS. To quantify the relative residue-specific trend, we used an established analysis method to scale the aggregation time (32, 33). For each set of aggregation data, LS-kinetics were fit to sigmoidal functions and the resulting t_{50}(LS) were used to scale the time axis (t/t_{50}) for all kinetics data ($n \geq 3$) (Figure 2). In accord with the unscaled data, smaller scaled t_{50} (t_{50}^{scaled}) values were observed when monitored by both Dns7 and Dns136 fluorescence ($t_{50}^{scaled}(\Delta\langle\lambda\rangle) = 0.870(3)$) compared to LS ($t_{50}^{scaled}$(LS) = 1.000(3), Table S2) while probes at positions 26 and 100 fully recapitulate the LS data [$t_{50}^{scaled}(\Delta\langle\lambda\rangle) = 0.990(3) \sim t_{50}^{scaled}$(LS) = 1.000(5)]. Our data suggest that the pathway for amyloid formation for the disordered N- and C-terminal regions develop initially from the ends, followed by residues towards the amyloid core (34).

The increased sensitivity of the N- and C-terminal distal sites may be coupled to the observation that in solution, these regions are involved in transient interactions (12–14,35,36). Particularly, if the preferred solution configuration is, either intraprotein (12,13) (C-to-NAC region, central hydrophobic region that is essential for aggregation) or antiparallel interprotein interaction (14) (N-to-C/C-to-N), then for α-syn to adopt a cross-β fold, where the β-strand residues are suggested to be parallel-in-register (N-to-C/N-to-C) (8,11,37), conformational rearrangement at the N- and C-termini must occur.

To shed light on the specific role of Dns7 and Dns136, we examined if the residue-specificity and sensitivity would be retained if we accelerated the lag phase by seeding with 3% WT fibrils (See Supporting Information for experimental details). Since α-syn aggregation kinetics can be described as a nucleation and nucleation dependent elongation mechanism (26–28), the observed early transition could reflect formation of intermediates or oligomers as well as initial filament elongation processes. Upon seeding, the lag phase will be significantly reduced and sometimes even abolished (38); thus, if the detected early events are related to nucleation, the observed differences between $t_{50}(\Delta\langle\lambda\rangle)$ and $t_{50}(\mathrm{LS})$ should diminish.

Consistent with spontaneous aggregation, the seeded samples showed earlier transitions for residues 7 and 136 ($t_{50}^{\mathrm{scaled}}(\Delta\langle\lambda\rangle) = 0.58(6)$ and 0.39(3), respectively (39), $t_{50}^{\mathrm{scaled}}(\mathrm{LS}) = 1.00(1)$, Figure 2 inset and Table S2). However, when monitored by Dns26 and Dns100 both showed identical fluorescence and LS kinetics data. Accordingly, we propose that these early conformational rearrangements likely occur after nucleation and represent filament formation or elongation processes.

In summary, our study has provided site-specific information on the role of the α-syn N- and C-termini in amyloid formation. Kinetics obtained for Dns fluorophores in the disordered (7 and 136) regions precede proximal (26 and 100) amyloid core sites. Both seeded and spontaneous aggregation kinetics suggest that residues 7 and 136 exhibit local conformational and environmental changes prior to, whereas changes for residues 26 and 100 occur concomitantly with, macroscopic fibril formation. Our results support the hypothesis that local structural reorganization at the N- and C-termini are necessary for α-syn to break the conformational constraints from either intra- or inter-polypeptide electrostatics attraction and thus, favor the formation of parallel, in-register, β-sheet fibrils.

Supplementary Material

Refer to Web version on PubMed Central for supplementary material.

Acknowledgments

We thank Mathew Daniels and Patricia Connelly (EM Core Facility), Greg Piszczek (Biophysics Facility) and Duck-Yeon Lee (Biochemistry Core) for technical assistance and Julie Maylor for synthesizing the Dns model complex.

References

1. Cookson MR. Annu Rev Biochem. 2005; 74:29–52. [PubMed: 15952880]
2. Uversky VN, Eliezer D. Curr Protein Pept Sci. 2009; 10:483–499. [PubMed: 19538146]
3. Seshadri S, Oberg KA, Uversky VN. Curr Protein Pept Sci. 2009; 10:456–463. [PubMed: 19538148]
4. Margittai M, Langen R. Q Rev Biophys. 2008; 41:265–297. [PubMed: 19079806]
5. Tompa P. FEBS J. 2009; 276:5406–5415. [PubMed: 19712107]
6. Tycko R. Q Rev Biophys. 2006; 39:1–55. [PubMed: 16772049]

7. Serpell LC, Berriman J, Jakes R, Goedert M, Crowther RA. Proc Natl Acad Sci USA. 2000; 97:4897–4902. [PubMed: 10781096]
8. Chen M, Margittai M, Chen J, Langen R. J Biol Chem. 2007; 282:24970–24979. [PubMed: 17573347]
9. Heise H, Hoyer W, Becker S, Andronesi OC, Riedel D, Baldus M. Proc Natl Acad Sci USA. 2005; 102:15871–15876. [PubMed: 16247008]
10. Qin Z, Hu D, Han S, Hong DP, Fink AL. Biochemistry. 2007; 46:13322–13330. [PubMed: 17963364]
11. Vilar M, Chou HT, Luhrs T, Maji SK, Riek-Loher D, Verel R, Manning G, Stahlberg H, Riek R. Proc Natl Acad Sci USA. 2008; 105:8637–8642. [PubMed: 18550842]
12. Bertoncini CW, Jung YS, Fernandez CO, Hoyer W, Griesinger C, Jovin TM, Zweckstetter M. Proc Natl Acad Sci USA. 2005; 102:1430–1435. [PubMed: 15671169]
13. Hoyer W, Cherny D, Subramaniam V, Jovin TM. Biochemistry. 2004; 43:16233–16242. [PubMed: 15610017]
14. Wu KP, Baum J. J Am Chem Soc. 2010; 132:5546–5547. [PubMed: 20359221]
15. Lee JC, Langen R, Hummel PA, Gray HB, Winkler JR. Proc Natl Acad Sci USA. 2004; 101:16466–16471. [PubMed: 15536128]
16. Pfefferkorn CM, Lee JC. J Phys Chem B. 2010; 114:4615–4622. [PubMed: 20229987]
17. Trexler AJ, Rhoades E. Biochemistry. 2009; 48:2304–2306. [PubMed: 19220042]
18. Ferreon ACM, Moran CR, Ferreon JC, Deniz AA. Angew Chem. 2010; 49:3469–3472. [PubMed: 20544898]
19. Dusa A, Kaylor J, Edridge S, Bodner N, Hong DP, Fink AL. Biochemistry. 2006; 45:2752–2760. [PubMed: 16489768]
20. Kaylor J, Bodner N, Edridge S, Yamin G, Hong DP, Fink AL. J Mol Biol. 2005; 353:357–372. [PubMed: 16171820]
21. Thirunavukkuarasu S, Jares-Erijman EA, Jovin TM. J Mol Biol. 2008; 378:1064–1073. [PubMed: 18433772]
22. van Rooijen BD, van Leijenhorst-Groener KA, Claessens MMAE, Subramaniam V. J Mol Biol. 2009; 394:826–833. [PubMed: 19837084]
23. Yushchenko DA, Fauerbach JA, Thirunavukkuarasu S, Jares-Erijman EA, Jovin TM. J Am Chem Soc. 2010; 132:7860–7861. [PubMed: 20491471]
24. Nath S, Meuvis J, Hendrix J, Carl SA, Engelborghs Y. Biophy J. 2010; 98:1302–1311.
25. Lakowicz, JR. Principles of fluorescence spectroscopy. 3. Springer; New York: 2006.
26. Morris AM, Watzky MA, Finke RG. Biochim Biophys Acta. 2009; 1794:375–397. [PubMed: 19071235]
27. Harper JD, Lansbury PT Jr. Annu Rev Biochem. 1997; 66:385–407. [PubMed: 9242912]
28. Wood SJ, Wypych J, Steavenson S, Louis JC, Citron M, Biere AL. J Biol Chem. 1999; 274:19509–19512. [PubMed: 10391881]
29. Ulmer TS, Bax A, Cole NB, Nussbaum RL. J Biol Chem. 2005; 280:9595–9603. [PubMed: 15615727]
30. We estimate the aggregation yield to be 80–90% assessed by UV spectroscopic analysis of the remaining soluble protein. While the absolute amount of β-sheet containing fibrils are difficult to determine, we find comparable CD spectroscopic signals (217–218 nm) as previous work (21).
31. Xue WF, Homans SW, Radford SE. Proc Natl Acad Sci USA. 2008; 105:8926–8931. [PubMed: 18579777]
32. Larson JL, Miranker AD. J Mol Biol. 2004; 335:221–231. [PubMed: 14659752]
33. Shim SH, Gupta R, Ling YL, Strasfeld DB, Raleigh DP, Zanni MT. Proc Natl Acad Sci USA. 2009; 106:6614–6619. [PubMed: 19346479]
34. Using similar analysis of the human islet amyloid polypeptide implicated in type 2 diabetes, the inner core residues showed earliest transitions while changes at residues on the N- and C-termini occurred later (33).
35. Lee JC, Gray HB, Winkler JR. J Am Chem Soc. 2005; 127:16388–16389. [PubMed: 16305213]

36. Allison JR, Varnai P, Dobson CM, Vendruscolo M. J Am Chem Soc. 2009; 131:18314–18326. [PubMed: 20028147]

37. Der-Sarkissian A, Jao CC, Chen J, Langen R. J Biol Chem. 2003; 278:37530–37535. [PubMed: 12815044]

38. Yagi H, Kusaka E, Hongo K, Mizobata T, Kawata Y. J Biol Chem. 2005; 280:38609–38616. [PubMed: 16162499]

39. The variations between seeded and spontaneous $t_{50}^{scaled}(\Delta\langle\lambda\rangle)$ obtained for Dns7 and Dns136 likely reflect the number and quality of the seeds introduced which are difficult to control. For example, when WT protein was seeded with 5% WT seed, we measured $t_{50}^{scaled}(\Delta\langle\lambda\rangle) = 0.45(2)$ for Dns7.

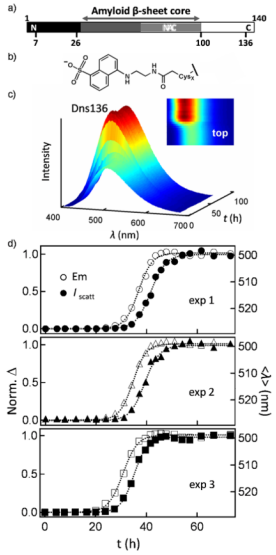

Figure 1.

(a) Primary sequence of α-syn highlighting the amyloid β-sheet core (residues 30-100), non-amyloid β component (NAC) region (residues 61-95), and Cys-labeling sites (G7C, V26C, L100C, Y136C) used in this study. (b) Structure of Dns fluorophore. (c) Representative fluorescence spectra of Dns136 (1.5 μM) during α-syn aggregation (100 μM in 25 mM NaPi, 100 mM NaCl, pH 7, 37 °C, shaking at 600 rpm, t = 0 – 75 h). *Inset* shows the Dns136 emission intensity surface. Dns emission intensity is in arbitrary units (blue-to-red) normalized to the highest intensity. Data for other sites can be found in Figure S3. (d) Aggregation kinetics for three independent measurements monitored simultaneously by Dns136 emission (Em, open symbols) and light scattering (I_{scatt}, closed symbols); typical lag phase ~ 20 – 30 h. Data for other sites can be found in Figure S7. Left axes represent normalized change (Norm. Δ) for I_{scatt} and Em and right axes represent absolute mean wavelength changes (<λ>).

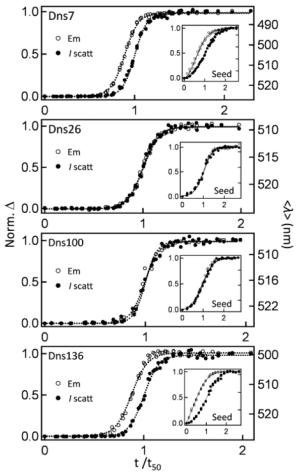

Figure 2.

Residue-specific probes of α-syn aggregation in the absence and presence (*Inset*) of preformed seeds (3%). Aggregation kinetics monitored simultaneously by Dns7, 26, 100, and 136 emission (Em, open circles) and light scattering (I_{scatt}, closed circles) for three independent measurements. To compare the different sites, we have normalized the time axes with I_{scatt} midpoint transition times (time that takes to reach 50% of maximum signal, t_{50}) extracted from fits of respective I_{scatt} data to sigmoidal functions. Left axes represent normalized change (Norm. Δ) and right axes represent absolute mean wavelength change (<λ>).